**PAPER • OPEN ACCESS**

# $^{80}$Se(n,$\gamma$) cross-section measurement at CERN n TOF

To cite this article: V. Babiano-Suarez *et al* 2020 *J. Phys.: Conf. Ser.* **1668** 012001



# $^{80}$Se(n,$\gamma$) cross-section measurement at CERN n_TOF

**V. Babiano-Suarez[g], O. Aberle[a], V. Alcayne[b], S. Amaducci[c,d], J. Andrzejewski[e], L. Audouin[f], M. Bacak[a,h,i], J. Balibrea-Correa[g], M. Barbagallo[a,j], S. Bennett[k], E. Berthoumieux[i], D. Bosnar[l], A. S. Brown[m], M. Busso[n,o], M. Caamaño[p], L. Caballero[g], M. Calviani[a], F. Calviño[q], D. Cano-Ott[b], A. Casanovas[q], F. Cerutti[a], E. Chiaveri[a,k], N. Colonna[j], G. P. Cortés[q], M. A. Cortés-Giraldo[r], L. Cosentino[c], S. Cristallo[n,s], L. A. Damone[j,t], P. J. Davies[k], M. Diakaki[u], M. Dietz[v], C. Domingo-Pardo[g], R. Dressler[w], Q. Ducasse[x], E. Dupont[i], I. Durán[p], Z. Eleme[y], B. Fernández-Domíngez[p], A. Ferrari[a], I. Ferro-Gonçalves[z], P. Finocchiaro[c], V. Furman[aa], R. Garg[v], A. Gawlik[e], S. Gilardoni[a], K. Göbel[ab], E. González-Romero[b], C. Guerrero[r], F. Gunsing[i], S. Heinitz[w], J. Heyse[ac], D. G. Jenkins[m], E. Jericha[h], U. Jiri[w], A. Junghans[ad], Y. Kadi[a], F. Käppeler[ae], A. Kimura[af], I. Knapová[ag], M. Kokkoris[u], Y. Kopatch[aa], M. Krtička[ag], D. Kurtulgil[ab], I. Ladarescu[g], C. Lederer-Woods[v], J. Lerendegui-Marco[r,g], S.-J. Lonsdale[v], D. Macina[a], A. Manna[ah,ai], T. Martínez[b], A. Masi[a], C. Massimi[ah,ai], P. F. Mastinu[aj], M. Mastromarco[a], E. Maugeri[w], A. Mazzone[j,ak], E. Mendoza[b], A. Mengoni[al,ah], V. Michalopoulou[a,u], P. M. Milazzo[am], M. A. Millán-Callado[r], F. Mingrone[a], J. Moreno-Soto[i], A. Musumarra[c,d], A. Negret[an], F. Ogállar[ao], A. Oprea[an], N. Patronis[y], A. Pavlik[ap], J. Perkowski[e], C. Petrone[an], L. Piersanti[n,s], E. Pirovano[x], I. Porras[ao], J. Praena[ao], J. M. Quesada[r], D. Ramos Doval[f], R. Reifarth[ab], D. Rochman[w], C. Rubbia[a], M. Sabaté-Gilarte[r,a], A. Saxena[aq], P. Schillebeeckx[ac], D. Schumann[w], A. Sekhar[k], A. G. Smith[k], N. Sosnin[k], P. Sprung[w], A. Stamatopoulos[u], G. Tagliente[j], J. L. Tain[g], A. E. Tarifeño-Saldivia[q], L. Tassan-Got[a,u,f], B. Thomas[ab], P. Torres-Sánchez[ao], A. Tsinganis[a], S. Urlass[a,ad], S. Valenta[ag], G. Vannini[ah,ai], V. Variale[j], P. Vaz[z], A. Ventura[ah], D. Vescovi[n,ar], V. Vlachoudis[a], R. Vlastou[u], A. Wallner[as], P. J. Woods[v], T. J. Wright[k], P. Žugec[l]**

[a] European Organization for Nuclear Research (CERN), Switzerland

[b] Centro de Investigaciones Energéticas Medioambientales y Tecnológicas (CIEMAT),Spain

[c] INFN Laboratori Nazionali del Sud, Catania, Italy
[d] Dipartimento di Fisica e Astronomia, Università di Catania, Italy
[e] University of Lodz, Poland
[f] IPN, CNRS-IN2P3, Univ. Paris-Sud, Université Paris-Saclay, F-91406 Orsay Cedex,France
[g] Instituto de Física Corpuscular, CSIC - Universidad de Valencia, Spain
[h] Technische Universität Wien, Austria
[i] CEA Saclay, Irfu, Université Paris-Saclay, Gif-sur-Yvette, France
[j] Istituto Nazionale di Fisica Nucleare, Bari, Italy
[k] University of Manchester, United Kingdom
[l] Department of Physics, Faculty of Science, University of Zagreb, Croatia
[m] University of York, United Kingdom
[n] Istituto Nazionale di Fisica Nazionale, Perugia, Italy
[o] Dipartimento di Fisica e Geologia, Università di Perugia, Italy
[p] University of Santiago de Compostela, Spain
[q] Universitat Politècnica de Catalunya, Spain
[r] Universidad de Sevilla, Spain
[s] Istituto Nazionale di Astrofisica - Osservatorio Astronomico d'Abruzzo, Italy
[t] Dipartimento di Fisica, Università degli Studi di Bari, Italy
[u] National Technical University of Athens, Greece
[v] School of Physics and Astronomy, University of Edinburgh, United Kingdom
[w] Paul Scherrer Institut (PSI), Villigen, Switzerland
[x] Physikalisch-Technische Bundesanstalt (PTB), Bundesallee 100, 38116 Braunschweig, Germany
[y] University of Ioannina, Greece
[z] Instituto Superior Técnico, Lisbon, Portugal
[aa] Joint Institute for Nuclear Research (JINR), Dubna, Russia
[ab] Goethe University Frankfurt, Germany
[ac] European Commission, Joint Research Centre, Geel, Retieseweg 111, B-2440 Geel,Belgium
[ad] Helmholtz-Zentrum Dresden-Rossendorf, Germany
[ae] Karlsruhe Institute of Technology, Campus North, IKP, 76021 Karlsruhe, Germany
[af] Japan Atomic Energy Agency (JAEA), Tokai-mura, Japan
[ag] Charles University, Prague, Czech Republic
[ah] Istituto Nazionale di Fisica Nucleare, Sezione di Bologna, Italy
[ai] Dipartimento di Fisica e Astronomia, Università di Bologna, Italy
[aj] Istituto Nazionale di Fisica Nucleare, Sezione di Legnaro, Italy
[ak] Consiglio Nazionale delle Ricerche, Bari, Italy
[al] Agenzia nazionale per le nuove tecnologie, l'energia e lo sviluppo economico sostenibile (ENEA), Bologna, Italy
[am] Istituto Nazionale di Fisica Nazionale, Trieste, Italy
[an] Horia Hulubei National Institute of Physics and Nuclear Engineering (IFIN-HH),Bucharest
[ao] University of Granada, Spain
[ap] University of Vienna, Faculty of Physics, Vienna, Austria
[aq] Bhabha Atomic Research Centre (BARC), India
[ar] Gran Sasso Science Institute (GSSI), L'Aquila, Italy

[as] Australian National University, Canberra, Australia

**Abstract.** Radiative neutron capture cross section measurements are of fundamental importance for the study of the slow neutron capture ($s$-) process of nucleosynthesis. This mechanism is responsible for the formation of most elements heavier than iron in the Universe. Particularly relevant are branching nuclei along the s-process path, which are sensitive to the physical conditions of the stellar environment. One such example is the branching at $^{79}$Se ($3.27\times10^5$ y), which shows a thermally dependent $\beta$-decay rate. However, an astrophysically consistent interpretation requires also the knowledge of the closest neighbour isotopes involved. In particular, the $^{80}$Se(n,$\gamma$) cross section directly affects the stellar yield of the "cold" branch leading to the formation of the $s$-only $^{82}$Kr. Experimentally, there exists only one previous measurement on $^{80}$Se using the time of flight (TOF) technique. However, the latter suffers from some limitations that are described in this presentation. These drawbacks have been significantly improved in a recent measurement at CERN n_TOF. This contribution presents a summary of the latter measurement and the status of the data analysis.

## 1. Astrophysical motivation and previous data

During the core He-burning and shell C-burning evolutionary stages of massive stars (M>8M$_\odot$), a large amount of neutrons are released via the $^{22}$Ne($\alpha$, n) reaction [1]. This activates nucleosynthesis of heavy elements with masses up to $A \sim 90$ on pre-existing Fe-seed nuclei. Long-lived radioactive nuclei ($T_{1/2} > 10$ y) may produce a split in the nucleosysnthesis path, thus producing a local isotopic abundance pattern that can be used to probe the physical conditions along different evolutionary stages, mainly during the $\sim$30 keV characteristic of He-burning and the $\sim$90 keV regime in C-burning [2].
In this contribution we focus on the $s$-process branching nucleus $^{79}$Se($T_{1/2} = 3.27(8)\times10^5$ y) [3], which has the peculiarity that it has a few quantum states at low excitation energy that are thermally populated in the stellar environment. $\beta$-decay from these states is much faster than from the ground state, thus changing the effective half-life and the strength of the branching according to the thermal conditions of the stellar environment (see Fig. 1). In this way, the abundance ratio of the $s$-only nuclei $^{80,82}$Kr, in combination with the $^{79}$Se(n,$\gamma$) cross section can be used to extract information about the thermal conditions of the environment [4].

In order to analyze this $s$-process branching reliably, one needs to know the neutron capture cross section of the $^{79}$Se(n,$\gamma$) reaction, as well as the neutron capture rates of the closest neighboring nuclei (see Fig. 1). A direct measurement of $^{79}$Se(n,$\gamma$) has been proposed for the experimental campaign of CERN after the present long shutdown (LS2) [6]. Preceding that experiment, several of the closest neighbours have been measured at CERN n_TOF, thereby covering also the main energy range of interest. In particular, $^{77,78}$Se(n,$\gamma$) were measured in other recent works[7]. This contribution presents the measurement and the status of the analysis for the $^{80}$Se(n,$\gamma$) data.

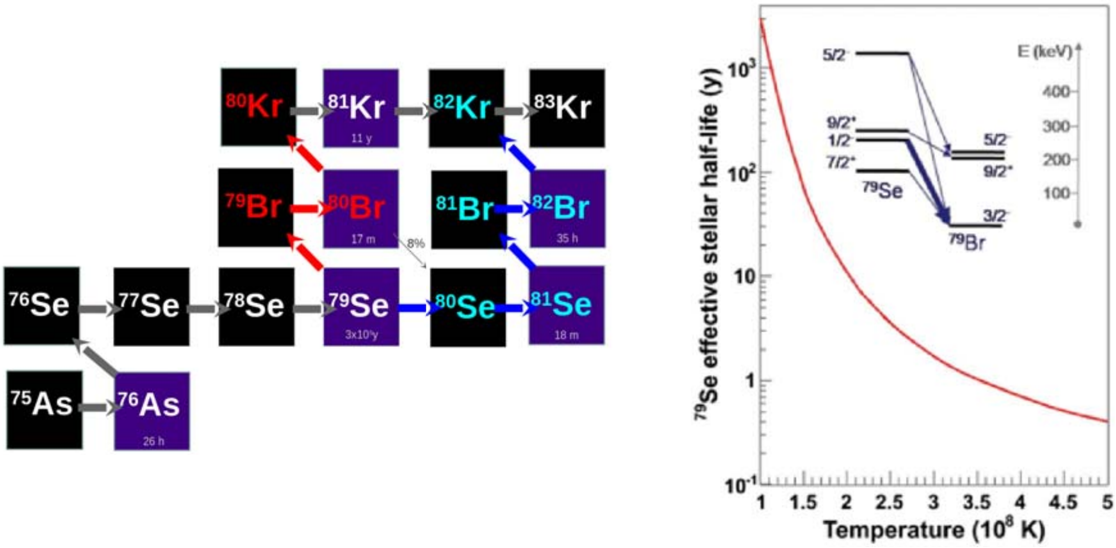


**Figure 1.** Nuclear chart and $s$-process path around the $^{79}$Se branching (left). Effective stellar half-life of $^{79}$Se as a function of the temperature (right) [5].

Regarding previous data, there exists only one previous TOF measurement on $^{80}$Se, which helped to constrain the physical conditions of the weak $s$-process [4]. However, the latter measurement suffers of some limitations that are explained in the following. On one hand, cross section data was obtained only beyond neutron energies of $\sim$3 keV. This prevented the measurement of one large $s$-wave resonance in the keV-region. While these resonances could barely affect the nucleosynthesis during the hot conditions of shell-carbon burning, they can play a crucial role during core He-burning, where temperatures of $\sim$ 30 keV are reached. Apparently, this effect is being neglected in present nucleosynthesis calculations. A second limitation of the previous experiment concerns the low energy resolution, which is due to the 60 cm flight-path used [4]. With the new experiment at CERN n_TOF these two aspects have been significantly improved. The new measurement was carried out at the EAR1 station, thereby covering a flight-path of 185 m. The long flight path in combination with the low duty-cycle (0.25 Hz) allows one to cover with high resolution the full neutron energy range from thermal up to several hundreds of keV. Although the neutron-energy differential capture cross section will be convolutioned with a Maxwell-Boltzmann distribution, a high TOF resolution becomes important to assess different experimental effects, such as to reliably account for contaminant isotopes in the sample. Finally, the set-up used in the previous experiment (see Fig. 3 in ref. [4]) may be of concern in terms of neutron-sensitivity bias for the resonances with large elastic scattering width $\Gamma_n$. Neutrons scattered in the sample at the energy of those resonances can be easily captured in the surrounding structural materials, thereby artificially enhancing the cross section. At n_TOF a big effort has been made in order to reduce as much as possible this type of background [8] [9]. An assessment of possible neutron-sensitivity deviations in our or previous experiments will be made in future stages of the data analysis.

Journal of Physics: Conference Series **1668** (2020) 012001 doi:10.1088/1742-6596/1668/1/012001



## 2. Methodology

For the measurement of $^{80}$Se(n,$\gamma$) we used a selenium sample enriched to 99.87% in $^{80}$Se. Two different pellets with masses of 0.966(2) g and 2.920(2) g and a diameter of 20 mm were produced at the Paul Scherrer Institute (PSI). The reason to produce two samples of different thicknesses was to have a more reliable assessment of the multiple scattering effects in the case of resonances with large scattering width $\Gamma_n$. The total number of protons used to measure these samples was $1.92\times10^{18}$, most of them dedicated to the heavier sample. More details are given in Table 1. Additional samples were also measured such as gold, lead and an empty frame. Gold was measured to apply the saturated resonance method [10], while lead and an empty frame were used to determine the measurement background. Furthermore, the neutron flux was monitored with a $^{6}Li$ foil intercepting the beam, and $^{3}$H products of the $^{6}$Li(n,$\alpha$) reaction were measured by using a silicon monitor placed off-beam.
For the TOF measurement we used the experimental area 1 (EAR1) of CERN n_TOF. Here, the pulsed neutron beam produced in the spallation target travels in high vacuum to reach the sample 185 m downstream. The time of flight is measured with a resolution of 2 ns using 500 MHz fast digitizers. The energy of neutrons is determined using the non-relativistic kinetic energy expression. When neutrons impinge on the sample, they can be captured thereby building compound nuclei. The latter are initially in an excited state, which de-excite by emitting a prompt cascade of gamma rays. By detecting this radiation one can determine the probability of a neutron to be captured by the sample depending on its energy, i.e. its neutron capture cross section.
In this experiment low efficiency $C_6D_6$ liquid scintillators were used to register the prompt capture gamma rays. Due to their low efficiency, at most one of the $\gamma$-rays from each cascade is recorded. For this reason, the Pulse Height Weighting Technique (PHWT) [11] has to be applied to the measured data. In this technique, a low detection efficiency and a proportionality between efficiency and energy of the detected gamma ray are required to avoid systematic bias in the final cross section due to the cascade multiplicity or decay path. More details can be found in [12]. The first condition is easy to achieve using low Z materials for the sensitive (small) volume of the detectors ($C_6D_6$ liquid scintillators). The second condition is not trivial and a weighting function has to be calculated, validated and applied to the detector response in order to make the efficiency proportional to the energy of the gamma ray. For an accurate use of the PHWT one needs to take into account several experimental effects, related with the low energy noise-discriminating threshold in the acquisition, with the $\gamma$-ray summing probability and other similar effects [12].

## 3. Preliminary Results

The n_TOF experimental weighted count rate as a function of the neutron energy is shown in Fig. 2 (red histogram) with an arbitrary scale. For comparison, the previous

**Table 1.** Number of protons dedicated for each sample measured during $^{80}$Se(n,$\gamma$) experiment.

| Sample | Mass (g) | Number of protons |
|---|---|---|
| $^{80}$Se | 2.920 | $1.824\times10^{18}$ |
| $^{80}$Se | 0.996 | $9.618\times10^{16}$ |
| $^{197}$Au | 0.644 | $2.136\times10^{17}$ |
| $^{Nat}$Pb | 7.281 | $1.164\times10^{17}$ |
| Empty | – | $5.091\times10^{17}$ |

cross section measurement [4] is also shown (blue dots). The aforementioned strong *s*-wave resonance below 3 keV can be observed, together with a narrower resonance at lower energy that can be unambiguously assigned to $^{80}$Se.
Previous to this result, a count rate consistency study was performed in order to detect possible discrepancies between count rates in the detectors. On it, ratios between count rates of $C_6D_6$ detectors and the silicon monitor were calculated. These ratios have to remain constant along the experiment, and any variation in the number of counts registered by the silicon monitor must also occur in the $C_6D_6$ detectors keeping the ratio between them constant. After this systematic study, a hundred percent of the total statistic was verified.
The weighted count-rate histogram shows an improvement of a factor of about 2 in signal-to-background ratio, when compared to the raw count-rate histogram. This is due to the "harder" nature of the capture gamma rays in selenium, when compared to the background radiation. In summary, over the full energy range of interest we have observed around 80 resonances from ∼eV up to ∼ 100 keV with sufficient statistics for a reliable R-matrix analysis. Next steps to complete the data analysis are summarized in the section below.

## 4. Summary and outlook

With the new measurement at CERN n_TOF one can claim that a significant improvement in terms of resolution and completeness has been achieved for the $^{80}$Se(n,$\gamma$) reaction with respect to previous data. The final results shall be relevant, together with other results in this mass region, towards a consistent interpretation of the branching at $^{79}$Se. The next steps to complete the analysis of $^{80}$Se(n,$\gamma$) are summarized in the following. Firstly, the weighting function needs to be validated on the basis of Monte-Carlo simulations of the capture cascade of $^{80}$Se+n, as reported in Ref. [12]. These simulations will serve also for the determination of the aforementioned threshold- and summing-correction factors. Secondly, the n_TOF weighted count-rate histogram needs to be converted to capture yield by using the neutron-energy dependent neutron flux of EAR1. A similar analysis of the background related runs shall allow us to evaluate the contribution of different background sources during the experiment. The capture

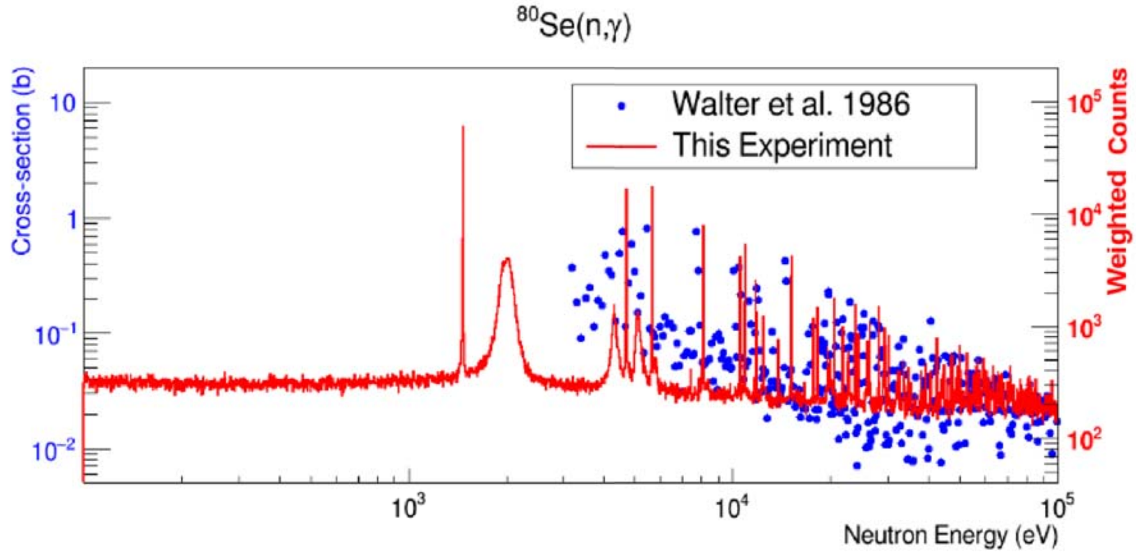


**Figure 2.** Experimental neutron energy spectrum in red, compared to available data of Walter et al. experiment in blue dots.

yield will be analyzed with an R-matrix code, such as SAMMY [13], in order to extract the cross section and the resonance parameters. Given the large number of resonances observed in the resolved resonance region, a statistical analysis will be performed in order to determine the level density and strength in $^{81}$Se. This information can be of interest in order to use the statistical nuclear model to extrapolate the cross section at higher neutron energy (beyond ∼100 keV).
Finally, we plan to carry out an astrophysical interpretation of the measured data using computational tools, such as those developed by NuGrid collaboration [14].

## 5. Acknowledgement

We acknowledge support from from the European Research Council (ERC) under the European Union's Horizon 2020 research and innovation program (grant agreement No. 681740), and the Spanish project FPA2017-83946-C2-1-P.

## References

[1] M. Pignatari et al., "The weak *s*-process in massive stars and its dependence on the neutron capture cross sections", The Astrophysical Journal, vol. 710, p. 1557-1577, 2010.

[2] F. Käppeler et al., "The *s*-process: Nuclear physics, stellar models and observations", Reviews of Modern Physics, vol. 83, p. 157, 2011.
[3] G. Jörg et al., "Preparation of radiochemically pure $^{79}$Se and highly precise determination of its half-life", vol. 68, p. 2339-2351, 2010.
[4] G. Walter et al., "The *s*-process branching at Se-79", Astronomy and Astrophysics, vol. 167, p. 186-199, 1986.
[5] K. Takahashi et al., "Nuclear $\beta$-decays of highly ionized heavy atoms in stellar interiors", Nuclear Physics, vol. 404, p. 578-598, 1983.
[6] C. Domingo-Pardo et al., CERN-INTC-2014-005. INTC-I-155, http://cds.cern.ch/record/1642787.
[7] C. Lederer et al., CERN-INTC-2017-038. INTC-P-509, http://cds.cern.ch/record/2265570.
[8] P. Zugec et al., "GEANT4 simulation of the neutron background of the $C_6D_6$ setup for capture studies at n_TOF", Nuclear Instruments and Methods in Physics Research Section A, vol. 760, p. 57-67, 2014.
[9] R. Plag et al., "An optimized $C_6D_6$ detector for studies of resonance-dominated (n,$\gamma$) cross-section", Nuclear Instruments and Methods in Physics Research Section A, vol. 496, p. 425-436, 2003.
[10] R.L. Macklin et al., "Absolute neutron capture yield calibration", Nuclear Instruments and Methods in Physics Research Section A, vol. 164, p. 213-214, 1979.
[11] R.L. Macklin et al., "Capture-Cross-Section Studies for 30-220 keV Neutrons Using a New Technique", Physical Review, vol. 159, p. 1007-1017, 1967.
[12] U. Abbondanno et al., "New experimental validation of the pulse height weighting technique for capture cross-section measurements", Nuclear Instruments and Methods in Physics Research Section A, vol. 521, p. 454-467, 2004.
[13] M. Larson, "SAMMY: Multilevel R-Matrix Fits to Neutron Data Using Bayes Equations", ORNL/TM-9179/R8 ENDF-364/R2, October 2008.
[14] Available online: "https://nugrid.github.io/".